Plain English and Japanese Summaries of

The 2011 M=9.0 Tohoku oki earthquake more than doubled the probability of large shocks beneath Tokyo

(in press, *Geophysical Research Letters*)

Shinji Toda

International Research Institute of Disaster Science (IRIDeS), Tohoku University, Japan

toda@irides.tohoku.ac.jp

Ross S. Stein

U.S. Geological Survey, Menlo Park (currently at the GEM Foundation, Pavia, Italy)

rstein@usgs.gov

東北地方太平洋沖地震により２倍以上に増加した東京の大地震発生確率

東北大学災害科学国際研究所
遠田晋次

米国地質調査所
ロス　スタイン

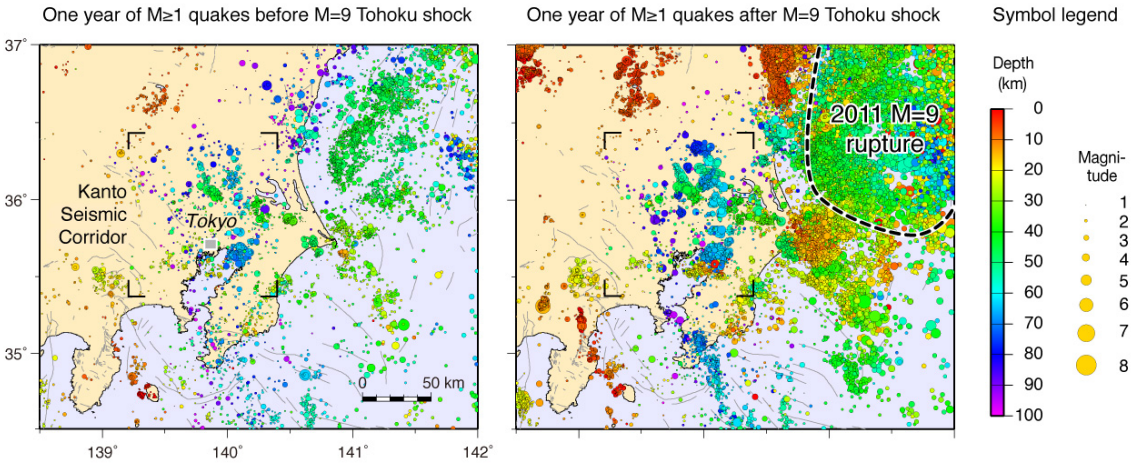

The Kanto seismic corridor surrounding Tokyo has been shaken by four to five Magnitude-7 or larger earthquakes since the founding of Edo (now Tokyo) in 1603, including the 1855 Magnitude~7.3 Ansei-Edo shock that all but destroyed the city. Thus in addition to infrequent great earthquakes along the Japan trench to the east and Sagami trough to the south, there is a local source of earthquakes beneath greater Tokyo.

The center of the 11 March 2011 Magntude-9.0 Tohoku oki rupture lies 300 km northeast of Tokyo, and its southernmost Magnitiude-7.9 aftershock lies 100 km northeast of Tokyo. Despite this great distance, the seismicity rate (the rate of Magnitude-3 and larger quakes) in the Kanto seismic corridor jumped by a factor of ten immediately after the M=9 earthquake. The seismicity rate decayed for 6-12 months, after which it steadied at three times the pre-Tohoku rate. The seismicity rate jump and decay to a new rate, as well as the near-shutdown of tensional earthquakes beneath Tokyo at the time of the Tohoku shock, can be explained by the stress imparted by the Tohoku rupture to the faults 60-80 km beneath the Kanto corridor. We therefore use a stress model to match the observations and to forecast the probability of large earthquakes in the corridor.

We estimate a 17% probability (1 chance in 6) of a Magnitude-7 or larger shock over the 5-year prospective period 11 March 2013 to 10 March 2018, two-and-a-half times the probability had the Tohoku earthquake not struck. For Magnitude-6.5 or larger shock, the probability rises from 18% before the mainshock to 41% afterwards, a similar probability gain. Thus, we argue that a three-fold increase in the rate of small shocks corresponds to a 2.6-fold increase in the probability of large ones. This forecast includes only earthquakes nucleating beneath Kanto; great Japan trench or Sagami trough events are also capable of strong shaking in the Kanto basin.

東北地方太平洋沖地震によって２倍増加した首都直下の大地震発生確率

東北大学災害科学国際研究所
遠田晋次

米国地質調査所
ロス　スタイン

東京（江戸）は，西暦 1603 年以来，直下で起こったマグニチュード（M） 7 以上の被害地震を４～５回経験しています．その中には，江戸に壊滅的な被害をもたらした 1855 年の安政江戸地震（M7.3）も含まれます．これらは主として，筑波山直下から千葉市にかけて南北に深さ 30km～80km の地震集中域（関東地震帯）から発生したと考えられます．房総半島東方沖の日本海溝や相模トラフ沿いの巨大地震と同様，関東地震帯は首都直下にあるプレート境界沿いで発生する「地震の巣」ともいえます．

東北地方太平洋沖地震の震源の中心は東京の約 300 km 北東に位置します．また，M7.6 の最大余震は東京の北東約 100 km で発生しました．これらの震源から距離があるにも関わらず，関東地震帯での１日あたりの地震数が普段の約 10 倍に増加しました．本震後半年～１年で地震発生ペースは急激に衰えましたが，１年後以降は普段の３倍のペースを保持しています．一方で，地殻が引っ張られたときに生じる地震（正断層型地震）は本震後ほぼ皆無となりました．これは，東北沖地震によって首都直下 60-80 km の深さに存在する断層へかかる力が変化したためです．このように，東北沖地震による首都直下の圧力変化とその後の地震活動が良く対応していることがわかったので，この関係を使って今後の大地震の予測を行いました．

我々の計算では，2013 年３月 11 日～2018 年同日までの５年間にマグニチュード７以上の地震が発生する確率は 17%です．これはサイコロを１回振ってある特定の数字が出る確率と同じです．東北沖地震が発生しなかった場合の 2.5 倍もの数字です．マグニチュード 6.5 まで考慮すると，その数字は仮に東北沖地震が発生しなかった場合は 18%ですが，同地震の影響を加えると 41%に上昇します．すなわち，小さな地震が３倍増えることで大地震の発生確率が 2.6 倍に増加することを意味します．今回の研究では，東京直下を含めた関東地震帯のみによるものですが，房総東方沖や相模トラフ沿いの巨大地震の可能性も今後考慮しなければなりません．

The 2011 M=9.0 Tohoku oki earthquake more than doubled the probability of large shocks beneath Tokyo

Shinji Toda[1] and Ross S. Stein[2]

[1] International Research Institute of Disaster Science (IRIDeS), Tohoku University, Japan

[2] U.S. Geological Survey, 345 Middlefield Rd, MS 977, Menlo Park, CA 94025, USA

Abstract. The Kanto seismic corridor surrounding Tokyo has hosted 4-5 M≥7 earthquakes in the past 400 years. Immediately after the Tohoku earthquake, the seismicity rate in the corridor jumped ten-fold, while the rate of normal focal mechanisms dropped in half. The seismicity rate decayed for 6-12 months, after which it steadied at three times the pre-Tohoku rate. The seismicity rate jump and decay to a new rate, as well as the focal mechanism change, can be explained by the static stress imparted by the Tohoku rupture and postseismic creep to Kanto faults. We therefore fit the seismicity observations to a rate/state Coulomb model, which we use to forecast the time-dependent probability of large earthquakes in the Kanto seismic corridor. We estimate a 17% probability of a M≥7.0 shock over the 5-year prospective period 11 March 2013 to 10 March 2018, two-and-a-half times the probability had the Tohoku earthquake not struck.

1. Introduction

We seek to understand the source and consequences of a remarkable increase in seismicity rate beneath greater Tokyo. Our goal is to transform these observations into a time-dependent occurrence probability of large, damaging earthquakes. The Kanto seismic corridor has produced many large damaging earthquakes since the founding of Edo (now, Tokyo) in AD

1603. These include the 1649 M~7.0, 1767 M~7.0, 1812 M~7.1, the Ansei-Edo 1855 M=7.1-7.4 that all but destroyed Tokyo, and 1856 M~6.8 earthquakes [*Grunewald and Stein*, 2006]. Although the depths of these events are unknown, and *Usami* [2003] provides somewhat different magnitudes and locations for them, the similarity of the intensity patterns for the 1855 Ansei-Edo earthquake and a 70-km-deep 2005 M=6.0 event near Chiba, suggests that the 1855 and 2005 events have similar hypocenters [*Bozkurt et al.*, 2007]. *Toda et al.* [2008] argued that these earthquakes, like the 40-80-km deep smaller shocks of the Kanto seismic corridor, are the product of the movement of a fragment of the Pacific slab wedged between the Pacific plate below and the Eurasian plate above. *Ishida* [1992] identifies what we regard as the Kanto fragment as a highly deformed Philippine Sea plate slab.

2. Seismicity Observations

Even though Tokyo lies 300 km southwest of the high slip portion of the M=9 rupture, and 100 km southwest of its M=7.9 aftershock (Figure 1a), the seismicity rate in the Kanto seismic corridor jumped by a factor of 10 immediately after the M=9 Tohoku earthquake (Figure 1b-c), as reported by *Toda et al.* [2011a], *Ishibe et al*. [2011], and *Hirose et al*. [2011]. The seismicity rate gain occurred at the same depth of pre-Tohoku shocks (Figure 1b-c). Maps of the seismicity rate change are shown in Figure S1; it is spatially quite stable.

The time series of M≥3 seismicity (Figure 2a) shows a steady background rate during 2006-2010, followed by a sudden jump and decay that resembles aftershock activity, evident at least to M≥5. Sometime during June-December 2011, the seismicity stopped decaying and has since remained constant (Figure 2b). This departure from the decay was not associated with any large Kanto shock (Figure 2a). The Kanto corridor earthquakes could be regarded as off-fault aftershocks of the Tohoku-oki earthquake. A decay exponent p of 0.44±0.07 would be needed to match their decay statistically with Omori process, about half a typical aftershock value. Even if the decay could be matched by Omori decay, the apparent background rate increase cannot. In contrast, the b-value for Kanto seismicity before the Tohoku mainshock is indistinguishable from that afterwards (Figure S2).

3. Static Coulomb Stress Model

Here we attempt to explain the observations by static stress transfer, seeking to explain the seismicity decay, the focal mechanism change, and the new background rate. The static Coulomb stress change caused by fault slip, $\Delta CFF = \Delta\tau + \mu'\Delta\sigma_n$, where $\Delta\tau$ is the shear stress change on the receiver (positive in the direction of presumed fault slip), $\Delta\sigma_n$ is the fault-normal stress change (positive when unclamped), and μ' is the effective coefficient of friction [*King et al.*, 1994; *Harris*, 1998]. We treat the 2011 source as an elastic dislocation in a halfspace with Young's modulus $8x10^5$ bar and Poisson's ratio 0.25, and resolve ΔCFF on 'receiver' faults identified from seismicity alignments, tomography and tectonic interpretation in *Toda et al.* [2008], or from focal mechanisms.

We use the 11 March 2011 M=9.0 source model of *Ide et al.* [2011] inverted from broadband seismic stations. We also include the Mw=7.9 aftershock, modeled as a simple tapered square following *Toda et al.* [2011b]. Because Kanto is so far from the 2011 rupture, the results are insensitive to the slip distribution; the stress transfer scales with the mainshock seismic moment and is most dependent on the inferred geometry and friction on the faults beneath Kanto. *Toda et al.* [2011b] tested friction coefficients of 0.0, 0.4, and 0.8 on the focal mechanisms of Tohoku aftershocks during March 2011, and found the best fit to the Coulomb stress change for 0.4, which we adopt here.

The 60- to 80-km-deep lower surface of the Kanto fragment is calculated to have been brought ~1 bar closer to failure (Figure 3), and its upper surface (not shown) 0.3 bar closer to failure [*Toda et al*., 2011b]. The Off-Boso portions of the Japan trench megathrust were also brought 2 bars closer to failure (Figure 3). Both regions experienced strong seismicity rate increases, with off-Boso gain higher than in the Kanto seismic corridor, consistent with the Coulomb modeling. The Off-Boso might be partially uncoupled, as assumed by Nishimura et al [*Uchida and Matsuzawa*, 2011].

To test whether the calculated stresses are responsible for the changes in seismicity rate and relative focal mechanism abundances, we next calculate the stress imparted to the 96 focal

mechanisms that occurred in the Kanto seismic corridor during the year after the mainshock, finding that 93% were brought closer to failure by the M=9.0 mainshock and M=7.9 aftershock. For non-zero friction, ΔCFF is dissimilar on the two nodal planes of each mechanism, so we randomly choose one plane of each pair. The significance of the 93% must be judged relative to a control population; for that we calculate stress from the 2011 mainshock to the 338 focal mechanisms in the same area before the mainshock, during 1997-2010, since these are unaffected by the Tohoku stress transfer. We randomly draw 96 mechanisms from this set 10,000 times and find that 78±8% (±2σ) were positively stressed (Figure 4c-d), and so the gain in promoted mechanisms is significant at more than 95% confidence. The gain arises in part because the rate of normal mechanisms dropped by half after the mainshock. Although earthquakes with normal mechanisms occurred in roughly the same locations and depths before the M=9 event and afterwards, the zone of post-Tohoku quakes is more restricted spatially than beforehand (dotted ellipses in Fig. 4). The change in the abundance of normal mechanism is significant at the 67% confidence level with respect to the 1997-2010 duration of the NIED F-net catalog (Figure S3). Thus, both the single-fault Kanto receiver of Figure 3, and the individual nodal planes of Figure 4, are consistent with stress transfer from the Tohoku-oki mainshock.

4. Rate/ State Coulomb Model of Seismicity Time Series

We therefore use the seismicity rate equation of rate/state friction of *Dieterich* [1994] to model the time-dependent response of seismicity to the static stress change on each nodal plane, following *Toda et al*. [2012]. In rate/state friction, a sudden stress increase amplifies the background rate, with the seismicity rate undergoing a step and decay resembling Omori aftershock decay, regardless of whether the shock is on or off the mainshock rupture surface. We calculate the rate/state evolution of seismicity caused by the static stress imparted to the nodal planes of all 338 pre-mainshock focal mechanisms; these are used as proxies of available nucleation sites. From the histogram of the stress changes on the nodal planes (Figure 2b inset), the mean increase of 1 bar is consistent with the simple planar model of Figure 3, but there is a range from -3 to +4 bar on the nodal planes**.** Most planes receive a stress increase from the 2011 mainshock, and so undergo a seismicity rate gain (Figure 2b,

light blue curves). But because of the diversity of strikes, dips, and rakes, some planes receive a stress decrease, and shut down (horizontal light blue lines). The predicted seismicity rate evolution of each of the 676 planes is shown as a light blue curve; their daily ensemble mean is the single dark blue curve.

In the initial model (blue curve in Figure 2b), we use the observed 2006-2010 background rate and fit the post-mainshock data with the constitutive parameter times the normal stress, $A\sigma$ (0.5 bar), and fault stressing rate $\dot{\tau}$ (0.25 bar/yr). The first post-Tohoku year is well fit, but the curve subsequently diverges from the observations. To fit the full time series, we increase $A\sigma$ to 0.6 bar, and include a stressing rate increase to 0.7 bar/yr at the time of the Tohoku earthquake (green curve in Figure 2b; individual time histories not shown). The values of $A\sigma$ needed to fit the decay, 0.5-0.6 bar, overlap the 0.4-0.5 bar found for California studies [*Toda et al*., 2005; *Toda et al*., 2012]. The stressing rates of 0.25-0.70 bar/yr are higher than in California studies.

5. Large Earthquake Probability Forecast

The ratio of small to large shocks, or b-value, is needed to transform the modeled rate of M≥3 earthquakes into the probability of M≥6.5 and M≥7.0 events; the lower the b-value, the higher the probability of large shocks. For Japan as a whole, b=0.9 (Figure S4). For the 3≤M≤6 earthquakes in the Kanto seismic corridor during 2009-2012, b=0.75, but the magnitude-frequency slope has a kink at M=4.1, which might be caused by the maximum 60-km depth of displacement magnitudes [*Harada et al*., 2004] (Figure S2). Over a slightly larger area, *Grunewald and Stein* [2005] found b=1.07 by combining instrumental earthquakes for 1923-2003 (4.5≤M≤6.5) with historical earthquakes since 1649 (6.6≤M≤7.4). For b=0.9 and the given the observed 0.15 M≥3/day earthquake rate before Tohoku, the M≥7 interevent time would be ~73 yr, in accord with the 400-yr record. If the M=4.1 kink were a real feature of the data, a b-value of 0.9 would project the rate of M≥3 shocks to M≥7.0. We thus regard b=0.75 as too low, b=0.9 likely, and b=1.0 possible.

The forecast rates and probabilities are given in Table 1. For b=0.9, the tripled earthquake rate results in a 5-yr M≥7 probability rising from 7% before the mainshock to 17% in the next 5 yr, a gain of 260%. For M≥6.5, the probability rises from 18% before the mainshock to 41% afterwards, a similar gain. Thus, a 3.0-fold increase in the M≥3 rate corresponds to a 2.6-fold increase in large earthquake probability. The gain is the same for b=1.0 but the probabilities are lower. The forecast includes only earthquakes nucleating beneath Kanto; M≥7.8 Japan trench or Sagami trough megathrust events are also capable of strong shaking in the Kanto basin.

6. Discussion and Conclusions

Because the Kanto seismicity did not decay back to the pre-Tohoku rate, we included a new stressing rate after the Tohoku mainshock, whose origin is uncertain. The most likely explanation is stress due to postseismic creep or viscoelastic rebound. From onland GPS data, *Ozawa et al.* [2012] identify two sources of postseismic megathrust creep, each with ≥1 m of slip (Figure 1a). On the basis of repeating earthquakes*, Uchida and Matsuzawa* [2013] infer that the patch near Choshi slipped ~0.5 m in the first 9 months after the mainshock. The eastern patch coincides with a ≥2-bar Coulomb stress increase caused by the 2011 mainshock (red zone in Figure 3). Slip of 1 m on these offshore sources would transfer 0.1-0.2 bar to the thrust faults beneath Kanto, increasing their stressing rate, although not enough to account for the modeled change from 0.25 bar/yr to 0.7 bar/yr. Viscoelastic relaxation could also increase the stressing rate.

There is a counter-argument to our claim of an increased earthquake probability: The post-Tohoku seismicity in the Kanto seismic corridor could simply accompany accelerated creep on uncoupled thrust faults beneath Kanto. *Uchida and Matsuzawa* [2013] infer fault slip on the Japan trench megathrust and in the Kanto seismic corridor from repeating earthquakes, estimating a 30 mm/yr slip rate in the Kanto seismic corridor during 1993-2010, and 320 mm slip from 11 March – 31 December 2011, or about 10 times the pre-Tohoku rate. This increase resembles the M≥3 time series in Figure 2b, which just means that the rate of the repeaters is proportional to the seismicity rate as a whole. The pre-Tohoku slip rate in the

Kanto seismic corridor inferred by *Uchida and Matsuzawa* [2013] is about the fragment motion rate deduced by *Toda et al.* [2008], implying that slip beneath Kanto could be fully uncoupled. If so, the accelerated post-Tohoku slip on corridor faults could shed—not increase—the stress imparted by Tohoku, much as a high rate of small shocks is seen along the creeping sections of the San Andreas fault.

But two observations make this alternative unlikely: First, there is a history of large earthquakes in the corridor. Among them, the 2005 M=6.0 shock struck at 80 km depth where the smaller shocks also occur, and so stress demonstrably accumulates on the corridor faults; they cannot be fully uncoupled. Second, the Kanto b-value did not change after the 2011 mainshock, and so Kanto is not experiencing a heightened rate of small shocks alone; the increased rate extends to M=6. Thus, in our judgment, the most defensible conclusion is that the corridor is at least partially coupled and accumulating stress; that the stress jumped in 2011 and is now being imparted at three times its foregoing rate; and so the probability of large shocks has climbed with the rate of small ones.

Acknowledgements. We thank Justin Rubinstein and Naoki Uchida for invaluable reviews. R.S.S. is grateful for a research visit to IRIDeS of Tohoku University, and S.T. is grateful for a research visit to the GEM Foundation, both in 2013. Coulomb 3.3 was used for stress calculations (www.coulombstress.org).

References

Bozkurt, S. B., Stein, R.S., and Toda, S. (2007), Forecasting probabilistic seismic shaking for greater Tokyo from 400 years of intensity observations, *Earthquake Spectra,* 23*,* 525-546, doi: 10.1193/1.2753504.

Dieterich, J. (1994), A constitutive law for rate of earthquake production and its application to earthquake clustering, *J. Geophys. Res*., 99, 2601–2618.

Frohlich, C. (1992), Triangle diagrams: ternary graphs to display similarity and diversity of earthquake focal mechanisms. *Phys. Earth and Planet. Int.* 75, 193-198, doi:110.1016/0031-9201(1092)90130-N.

Grunewald, E., and R.S. Stein (2006), A new 1649–1884 catalog of destructive earthquakes near Tokyo and implications for the long‐term seismic process, *J. Geophys. Res*., 111, B12306, doi:10.1029/2005JB004059.

Harada, S., H. Ueno, and H. Ohno (2004), The New Japan Meteorological Agency (JMA) Magnitude, Japan Geoscience Union (JPGU) meeting abstract, http://www2.jpgu.org/meeting/2004/pdf/s050/s050-004_e.pdf.

Harris, R. A. (1998), Introduction to special section: Stress triggers, stress shadows, and implications for seismic hazard, *J. Geophys. Res.*, 103, 24,347–24,358.

Hirose, F., K. Miyaoka, N. Hayashimoto, T. Yamazaki, and M. Nakamura (2011), Outline of the 2011 off the Pacific coast of Tohoku Earthquake (M_w 9.0)—Seismicity: foreshocks, mainshock, aftershocks, and induced activity, *Earth Planets Space,* 63, 513-518, doi:10.5047/eps.2011.05.019.

Ide, S., A. Baltay, and G. Beroza (2011), Shallow dynamic overshoot and energetic deep rupture in the 2011 M_w 9.0 Tohoku-Oki earthquake, *Science*, 332, doi: 10.1126/science.1207020.

Ishibe, T., K. Shimazaki, K. Satake, and H. Tsuruoka (2011), Change in seismicity beneath the Tokyo metropolitan area due to the 2011 off the Pacific coast of Tohoku Earthquake, *Earth Planets Space*, 63, 731–735, 201, doi:10.5047/eps.2011.06.001.

Ishida, M. (1992), Geometry and relative motion of the Philippine Sea plate and Pacific plate beneath the Kanto-Tokai district, Japan. *J. Geophys. Res*. 97, 489–513.

Nishimura, T., T. Sagiya, and Stein, R.S. (2007), Crustal block kinematics and seismic potential of the northernmost Philippine Sea late and Izu microplate, central Japan, inferred from GPS and leveling data, *J. Geophys. Res.,* 112, doi:10.1029/2005JB004102.

King, G.C.P., R.S. Stein, and J. Lin (1994), Static stress changes and the triggering of earthquakes, *Bull. Seismol. Soc. Am*., 84, 935–953.

Ozawa, S., T. Nishimura, H. Munekane, H. Suito, T. Kobayashi, M. Tobita, and T. Imakiire (2012), Preceding, coseismic, and postseismic slips of the 2011 Tohoku earthquake, Japan, *J. Geophys. Res.,* 117, B07404, doi:10.1029/2011JB009120.

Toda, S., R.S. Stein, K. Richards-Dinger, and S. Bozkurt (2005), Forecasting the evolution of seismicity in southern California: Animations built on earthquake stress transfer, *J. Geophys. Res*., *110*, B05S16, doi:10.1029/2004JB003415.

Toda, S., R.S. Stein, S. H. Kirby, and S. B. Bozkurt (2008), A slab fragment wedged under Tokyo and its tectonic and seismic implications, *Nature Geoscience*, 1, 771–776, doi:10.1038.ngeo318.

Toda, S., R.S. Stein, and J. Lin (2011a), Widespread seismicity excitation throughout central Japan following the 2011 M=9.0 Tohoku earthquake, and its interpretation by Coulomb stress transfer, *Geophys. Res. Lett.,* 38, L00G03, doi:10.1029/2011GL047834.

Toda, S., J. Lin, and R. S. Stein (2011b), Using the 2011 M=9.0 Tohoku earthquake to test the Coulomb stress triggering hypothesis and to calculate faults brought closer to failure, *Earth Planets Space*, 63, 1-6, doi:10.5047/eps.2011.05.010,

Toda, S., R.S. Stein, G.C. Beroza, and D. Marsan (2012), Aftershocks halted by static stress shadows, *Nature Geoscience, 5*, 410-413, doi:10.1038/ngeo1465.

Uchida, N., and T. Matsuzawa (2011), Coupling coefficient, hierarchical structure, and earthquake cycle for the source area of the 2011 off the Pacific coast of Tohoku earthquake inferred from small repeating earthquake data, *Earth Planets Space*, 63, 675–679, doi:10.5047/eps.2011.07.006.

Uchida, N., and T. Matsuzawa (2013), Pre- and post-seismic slow slip surrounding the 2011 Tohoku-Oki earthquake rupture, *Earth Planet. Sci. Lett*., in press.

Usami, T. (2003), Materials for Comprehensive List of Destructive Earthquakes in Japan (in Japanese), 605 pp., Univ. of Tokyo Press, Tokyo.

Table 1. Probabilities of large earthquakes striking greater Tokyo (the Kanto seismic corridor) during the next five years (11 Mar 2013-10 Mar 2018) and next year (11 Mar 2013-10 Mar 2014)

	Pre-M9 Tohoku mainshock			Post-M9 Tohoku mainshock				
	Ann. Rate	5-yr Prob. (%)	1-yr Prob. (%)	Ann. Rate	5-yr Prob. (%)	5-yr Prob. gain (%)	1-yr Prob. (%)	1-yr Prob. gain (%)
M≥6.5								
b = 0.9	0.039	17.6	3.8	0.106	41.3	235	10.1	266
b = 1.0	0.017	8.3	1.7	0.048	21.1	254	4.6	271
M≥7.0								
b = 0.9	0.014	6.6	1.4	0.038	17.2	261	3.7	264
b = 1.0	0.005	2.7	0.5	0.015	7.2	267	1.5	300

Probability, $P = 1 - \exp(-N)$, where N is the expected number of events. N = Ann. Rate x years. This estimate excludes earthquake sources on the Japan trench or Sagami tough megathrusts.

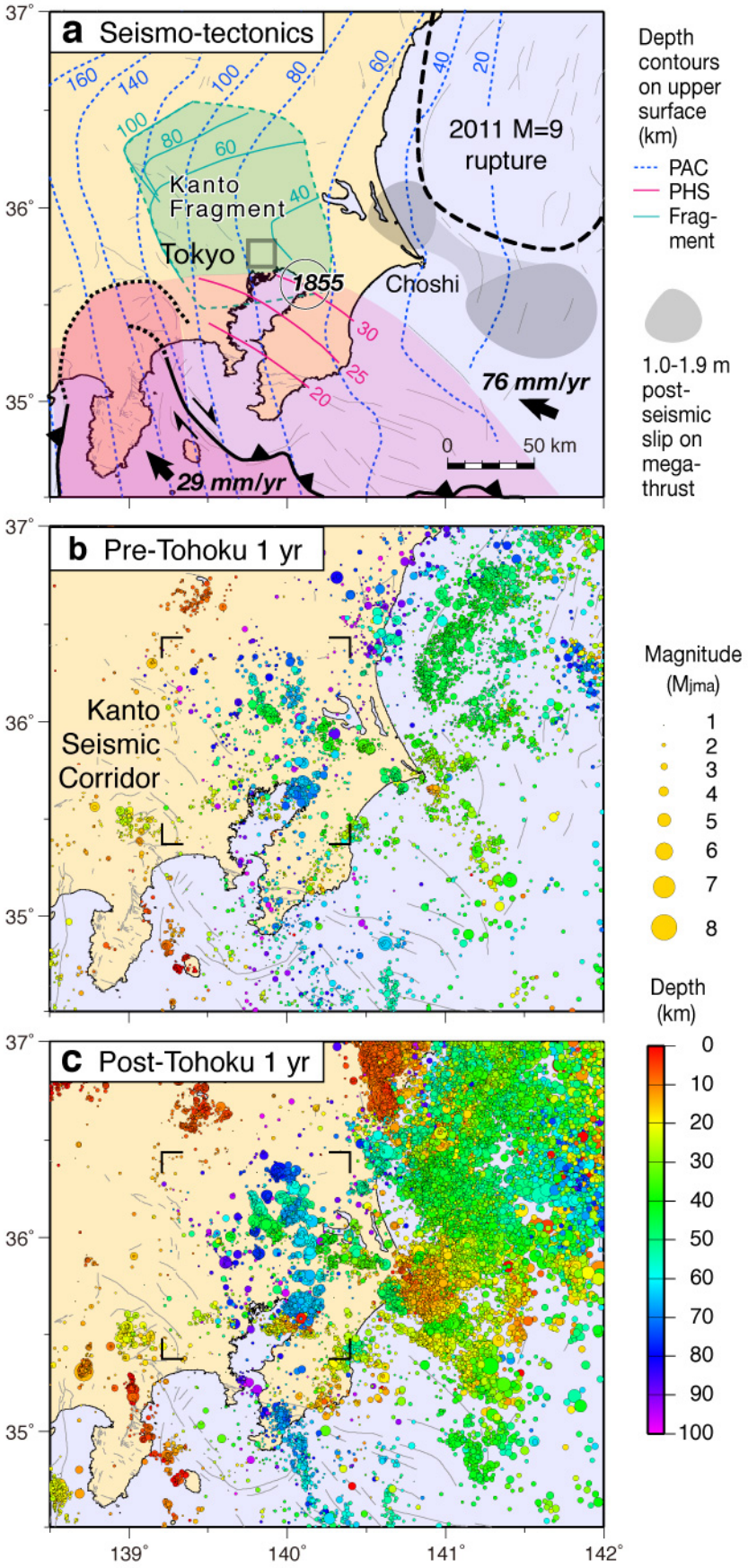

Figure 1. (a) Tectonic interpretation from Toda et al. [2008], showing the juxtaposition of the Pacific (PAC) and Philippine Sea (PHS) plates, and the 'Kanto fragment,' and the sites of post-Tohoku megathrust slip from Ozawa et al. [2012]. (b-c) Map of M≥1 seismicity during the year before (b) and after (c) the M=9 Tohoku quake.

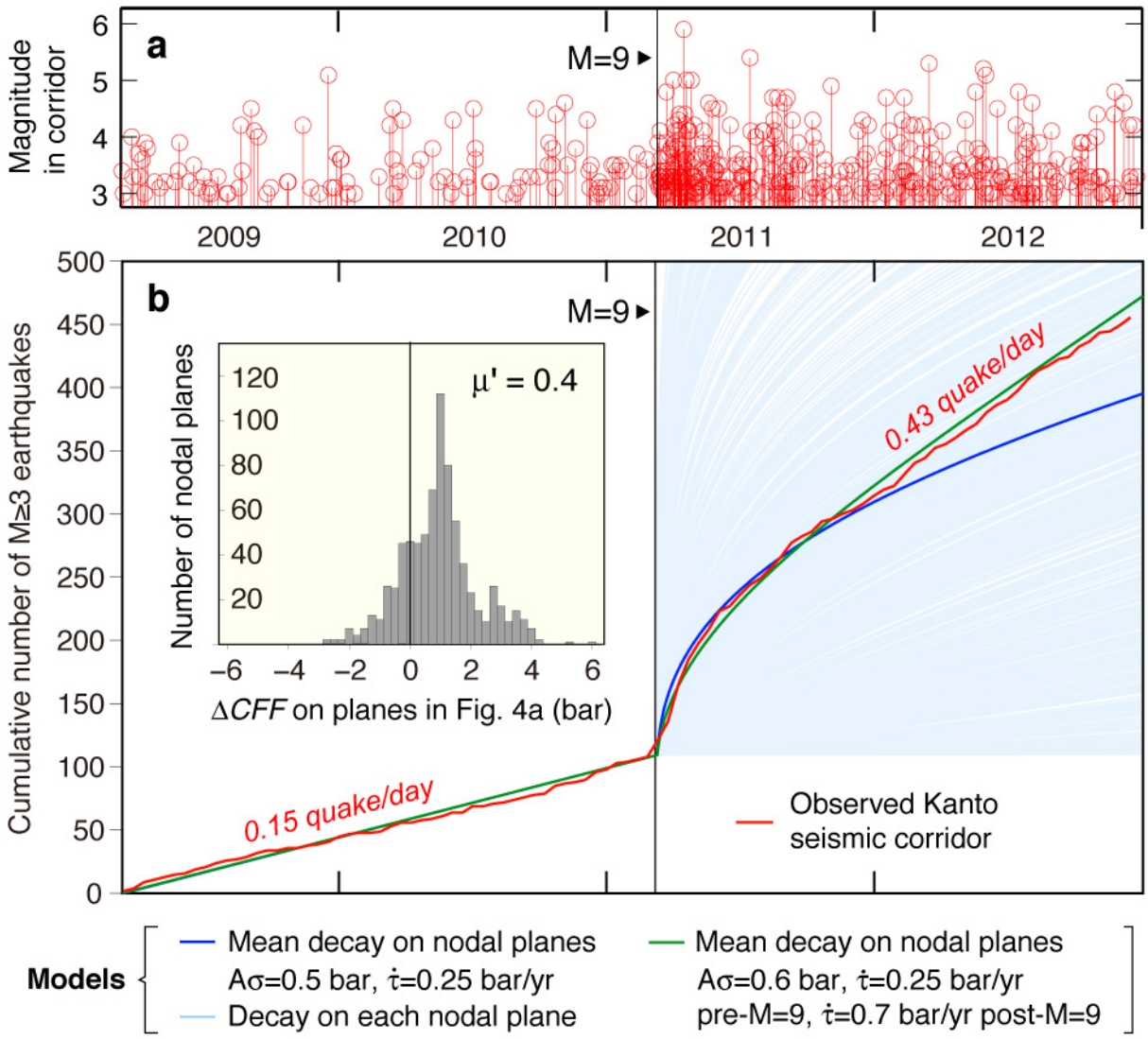

Figure 2. Change in earthquake rate in the Kanto seismic corridor. (a) Time series of M≥3 shocks, for which completeness is well below M=3 for all times, based on plots such as Fig. S2. (b) Cumulative M≥3 earthquakes, with initial (blue) and revised (green) models. Nodal planes during the pre-Tohoku period (Figure 4a) are taken to represent potential rupture sites; the stress imparted by the Tohoku shock should activate some and shut down others. ΔCFF on both nodal planes of each of the 388 mechanisms is calculated and the Dieterich [1994] seismicity-rate equation is evolved for each plane and plotted as light blue curves. The green curve also includes a stressing rate change at the time of the M=9.0 shock.

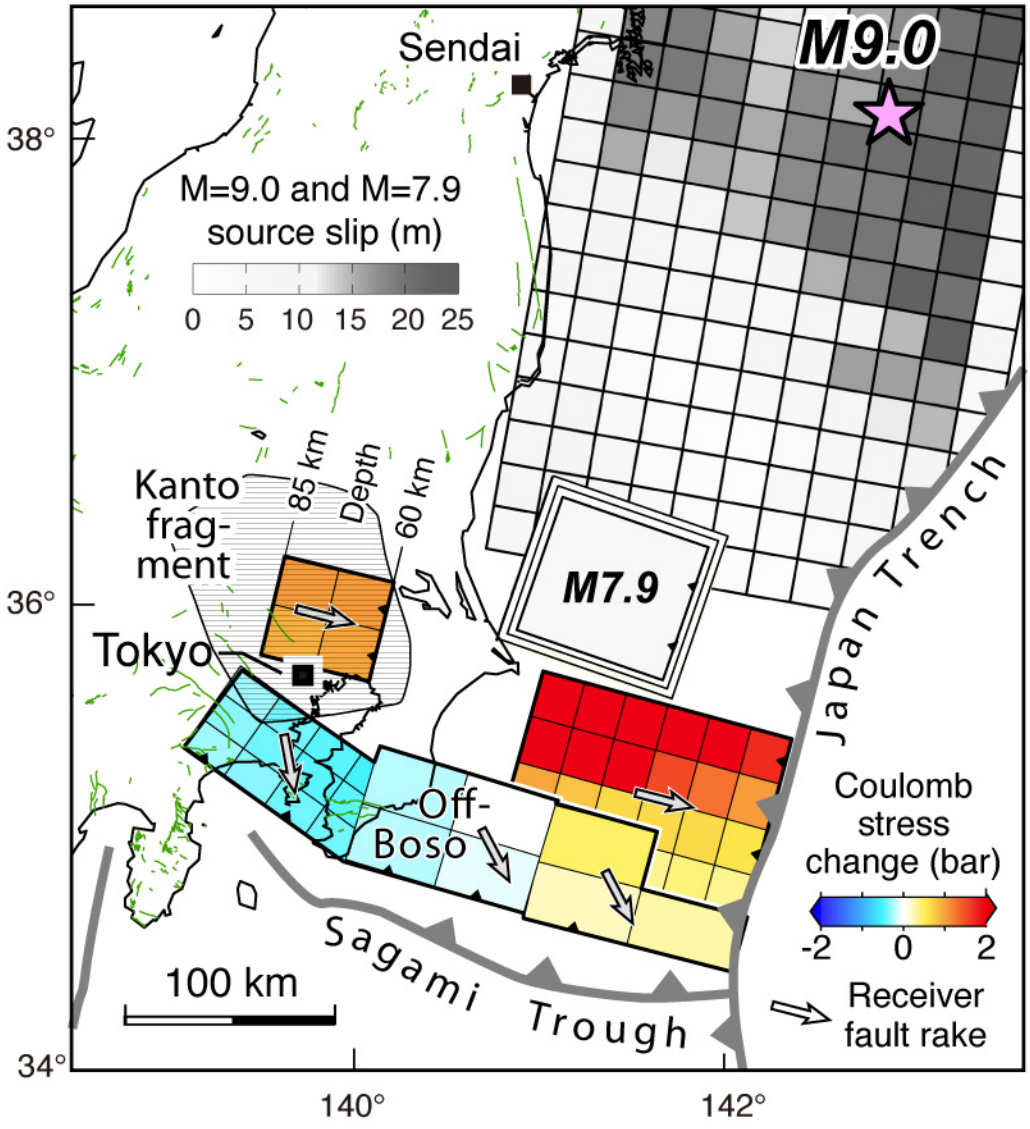

Figure 3. Tohoku-oki earthquake source geometry and slip from Ide et al. [2011] is used to calculate stress imparted to faults surrounding Tokyo. The Kanto fragment, southernmost portion of the Japan Trench megathrust, and easternmost portions of the Sagami troigh megathrust, are brought closer to failure.

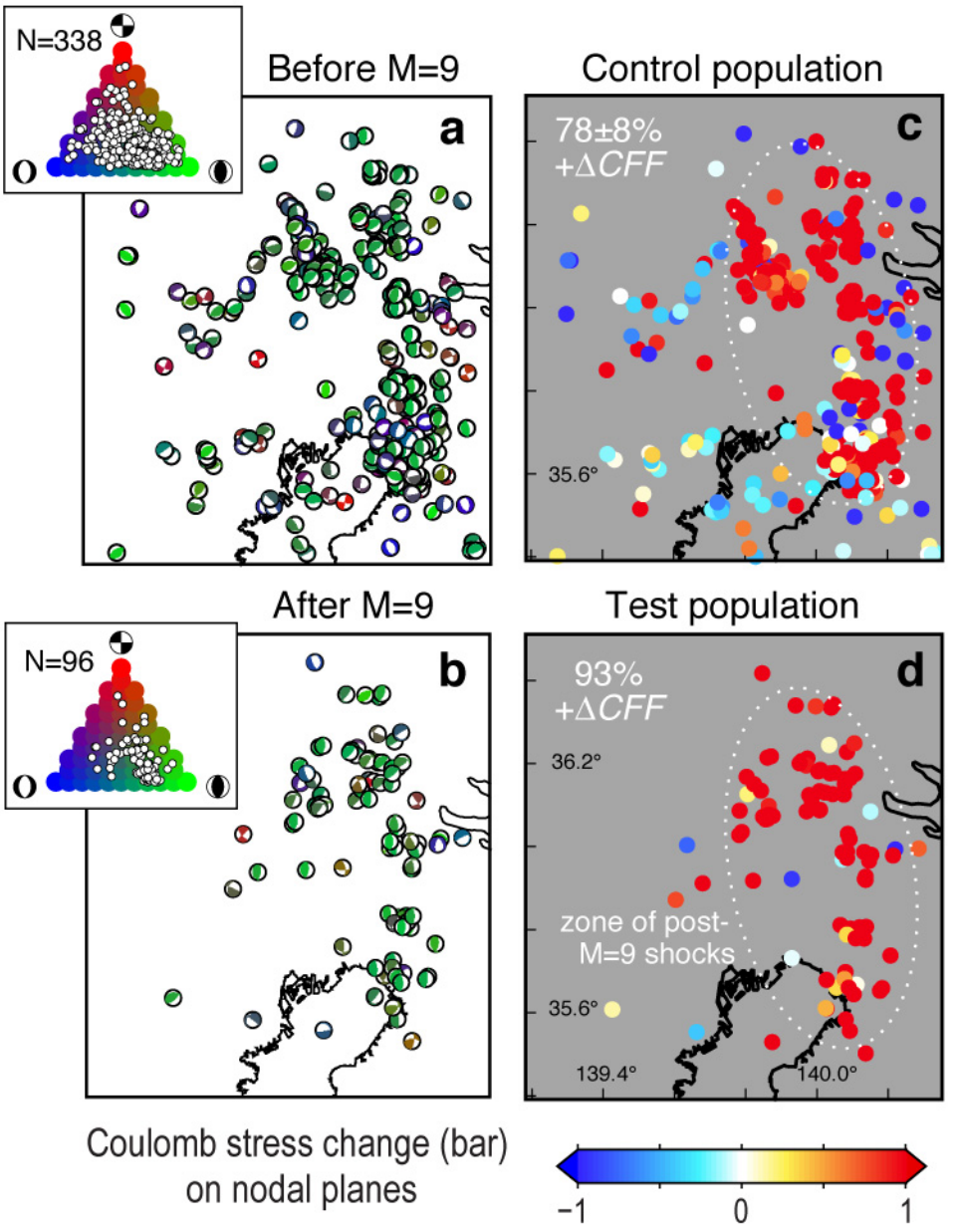

Figure 4. Focal mechanisms at 0-100 km depth from K-net in the Kanto area during 1997-2010 (a) and during one year after the Tohoku earthquake (b); the inset ternary diagrams, following Frolich [1992], show the mechanism distribution. (c) Coulomb stress, for friction of 0.4, imparted by the M=9 mainshock resolved on the focal mechanisms of the Kanto earthquakes that occurred before (c) and after (d) Tohoku.

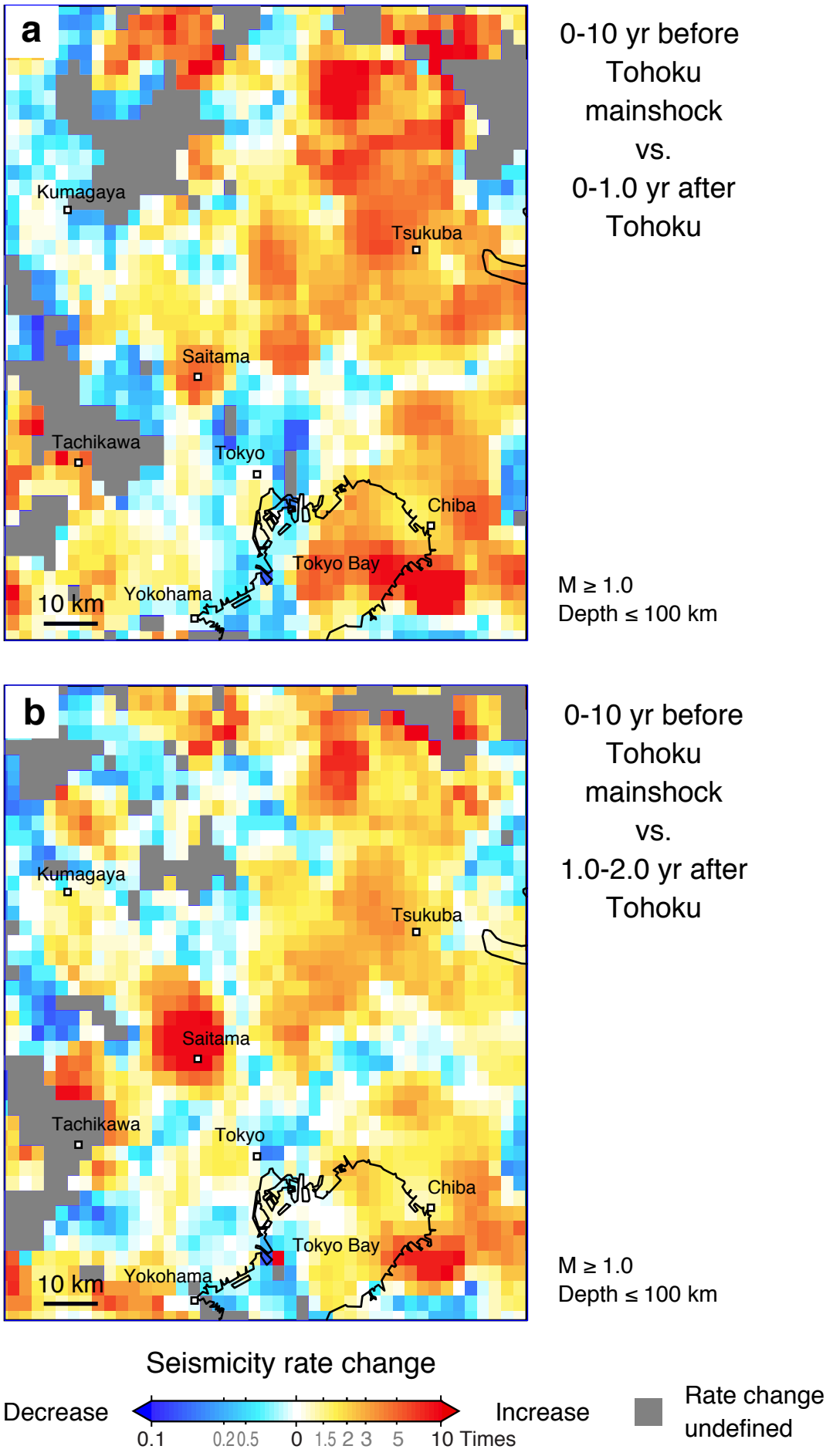

Figure S1. Map of the seismicity rate, using a 5-km-radius Gaussian smoothing kernel, showing a broad post-Tohoku increase, both immediately after the mainshock (a), and also once the rate change became steady (b).

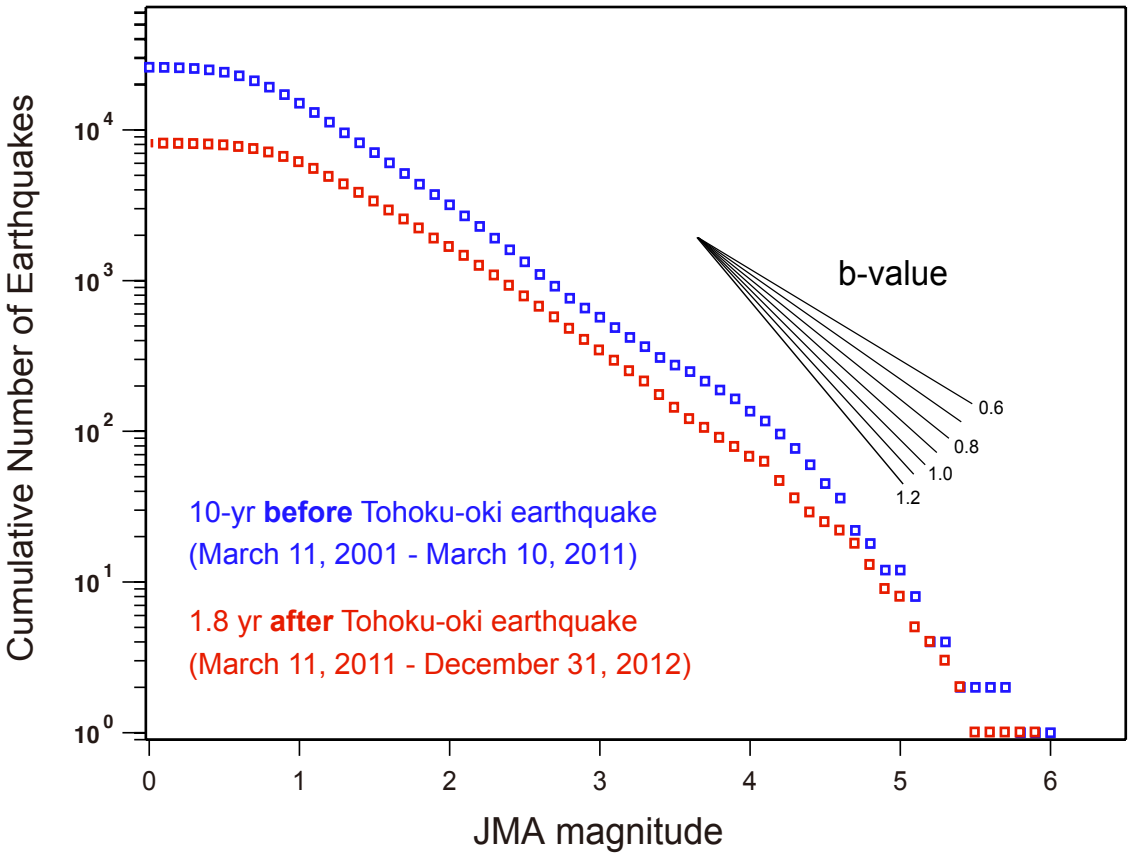

Figure S2. Magnitude-frequency plots for the Kanto seismic corridor (area shown in Figure 2, depth ≤100 km) before and after the Tohoku mainshock. There is little or no change in b-value. A kink in the magnitude-frequency slope at M~4.1 is also evident; b for M≤4.1 ~0.7, and be for M>4.1 ~0.9. The magnitude of completeness, Mc≤1.5 for all but the first weeks after the M=9 shock. Projecting from M=3 to M=7.0 would yield an effective b-value of 0.9.

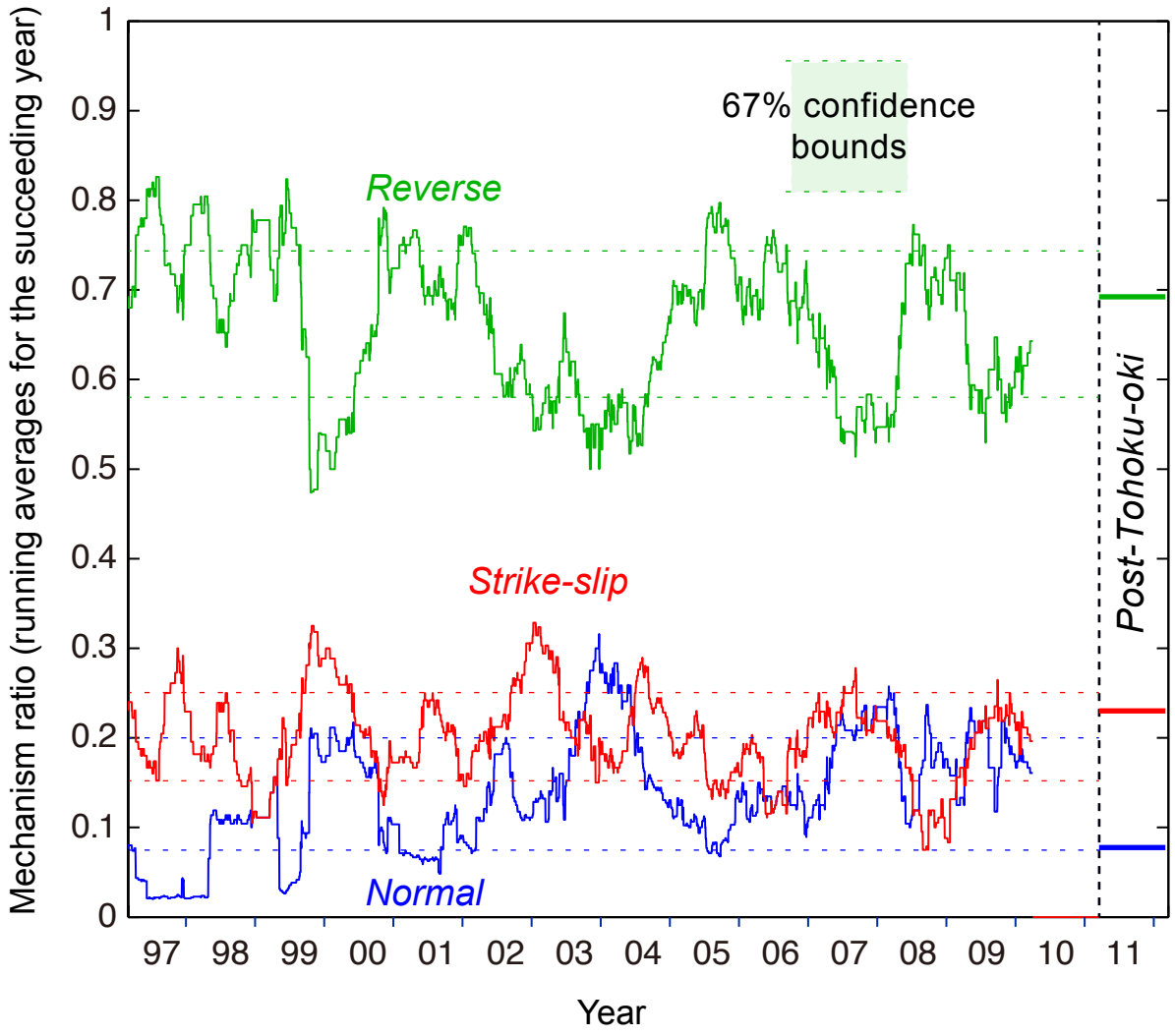

Figure S3. Ratio of mechanisms in the Kanto seismic corridor from 1997-2012, from the F-net catalog. After the Tohoku shock, the rate of normal mechanisms declined to a level at the 67% confidence range.

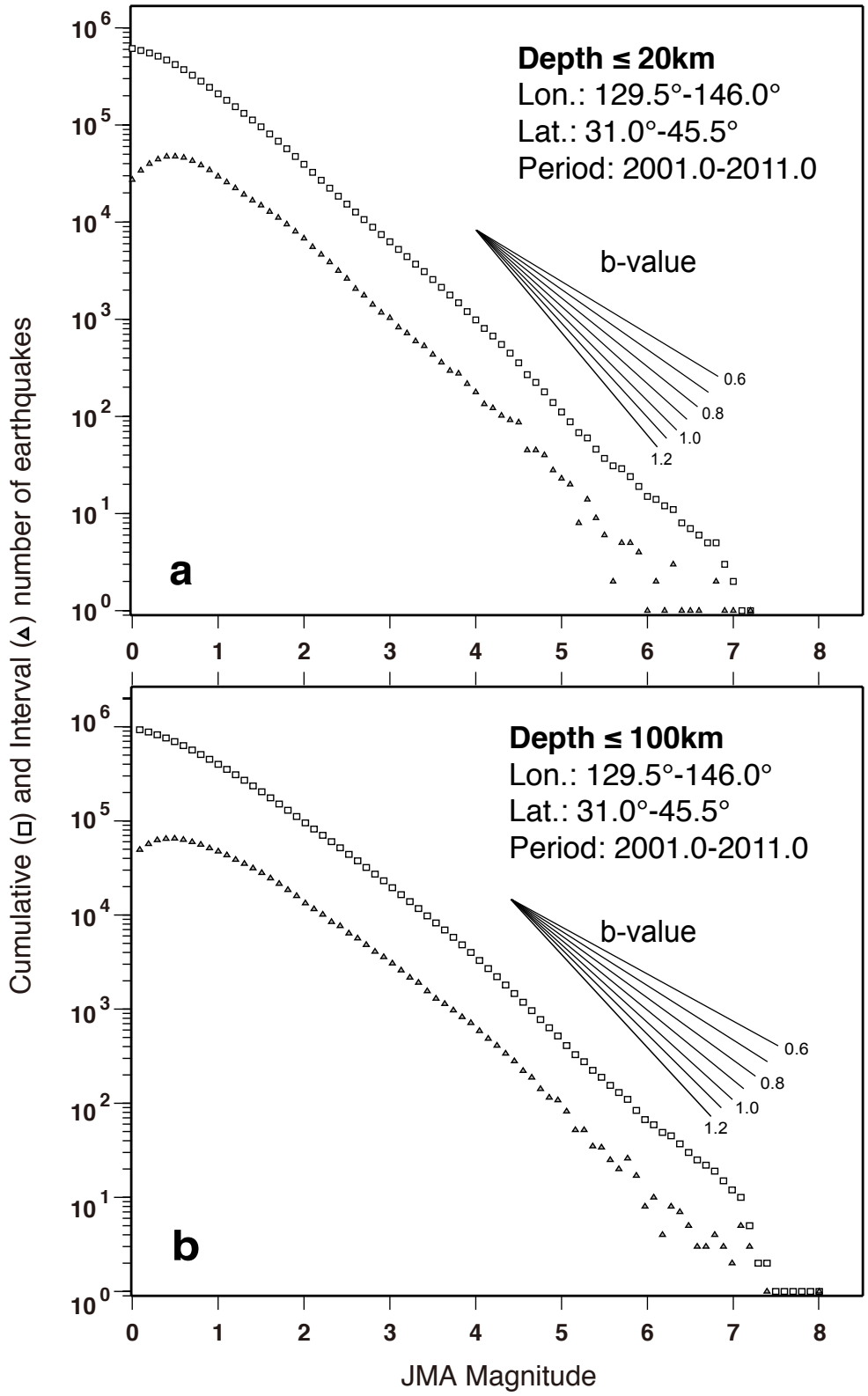

Figure S4. Magnitude-frequency plots for all of Japan, calculated for shallow earthquakes (a) and those above 100 km depth (b). The b-value is 0.9 for M≥4.0.